Computational homogenization of periodic beam-like structures

Patrice Cartraud, Tanguy Messager

Computational homogenization of periodic beam-like structures

Patrice Cartraud, Tanguy Messager

Institut de Recherche en Génie civil et Mécanique (GeM), UMR CNRS 6183 Ecole Centrale de Nantes, BP 92101, 44321 Nantes cédex 3, France

This paper is concerned with the computation of the effective elastic properties of periodic beam like structures. The homogenization theory is used and leads to an equivalent anisotropic Navier Bernoulli Saint Venant beam. The over all behavior is obtained from the solution of basic cell problems posed on the three dimensional period of the structure and solved using three dimensional finite element implementation.

This procedure is first applied to two corrugated zigzag and sinus beams subjected to in plane loading. Next, the axial elastic properties of a stranded '6 + 1' wire cable are computed. The effective properties values obtained appear to be very close to analytical reference results showing the efficiency of the approach.

1. Introduction

Beam-like structures with periodic microstructure may be found in various engineering applications, e.g., reinforced concrete beams, repetitive lattice beams and trusses and stranded ropes. The use of homogenized beam models offers a practical and efficient approach for analyzing such structures, resulting in a large reduction in the number of degrees of freedom. Several methods are discussed in the literature for the global modeling of periodic beams: some of them are restricted to lattice structures as studied by Noor (1988), to simple geometries (transfer matrix methods, see Stephen and Wang, 1996), or to microstructures which may be described as a lattice of curved-beam elements as studied by Potier-Ferry and Siad (1992).

Homogenization theory appears to be a more powerful method, since it can be applied to microstructure of general shape, and arbitrary heterogeneity. Using this method, the initial three-dimensional heterogeneous problem splits in a microscopic three-dimensional problem posed on the basic cell of the structure and a macroscopic beam problem. The microscopic analysis provides the beam's overall stiffness.

In the literature, the application of the method to practical situations appears to be limited, especially by means of a numerical approach. This paper presents a numerical implementation of the method, the computation of the effective beam properties being performed using a finite element analysis of the basic cell problems. First, the computation of the static in-plane stiffness of two corrugated (having sinus and zigzag mean-lines) beams is presented. Thereafter, the axial behavior of an helical cable is investigated. The accuracy of the approach is assessed with respect to analytical reference solutions of the literature.

The summation convention on repeated indices will be used throughout the paper. The Latin indices range from 1 to 3, whereas the Greek indices range from 1 to 2. Dots and semi-colons denote the scalar and double products of tensors, e.g., $(\sigma.n)_i \quad \sigma_{ij}n_j$ and $(a{:}e)_{ij} \quad a_{ijkl}e_{kl}$.

2. The homogenization method

2.1. Theoretical aspects

The homogenization theory, based on the asymptotic expansion method, has mainly be used for prismatic homogeneous or composite beams as detailed by Trabucho and Viaño (1996) and Volovoi et al. (1999). In such applications, the small parameter e is defined as the slenderness of the structure (the ratio of the width of the cross-section to the total length of the beam). Moreover, for beams with periodic microstructure, the ratio of the length of the period to the total length of the beam is a second small parameter denoted ε (see Fig. 1). The purpose of homogenization is then to substitute the actual three-dimensional heterogeneous and slender domain with an homogeneous beam, by making the two small parameters e and ε tend to zero. This problem was studied theoretically by Geymonat et al. (1987), where it was shown that different effective stiffnesses can be obtained in the case of a beam with variable cross-section, depending on the order in which the two small parameters tend to zero: namely, $\varepsilon \to 0$ first, and then $e \to 0$, or $e \to 0$ first, and then $\varepsilon \to 0$ (see also Cioranescu and Saint Jean Paulin, 1999 for reticulated structures). Another way to proceed is to assume that $e \to 0$ and $\varepsilon \to 0$ simultaneously. This latter method has been initially presented in Kolpakov (1991) (see also Kalamkarov and Kolpakov, 1997; Buannic and Cartraud, 2001; Kolpakov, 2004), as an extension of the work of Caillerie (1984) for periodic plates.
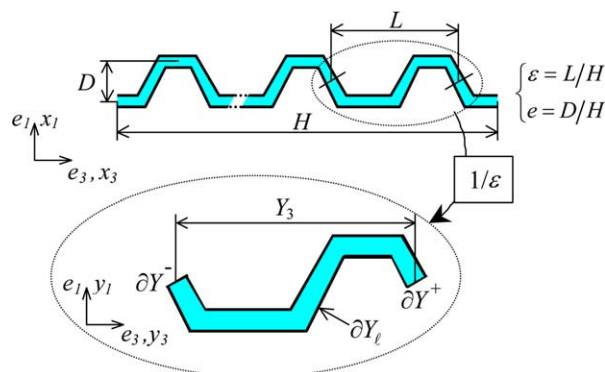

Fig. 1. The periodic structure and its basic cell.

Thus, three homogenization approaches are available, with their own domain of validity. Our objective here is not to discuss these different methods, the interested reader is referred to Buannic and Cartraud (2001) (and references herein) for periodic beams : it turns out that the most accurate effective properties are obtained when $e \to 0$ and $\varepsilon \to 0$ simultaneously, the only restrictions being $e \ll 1$ and $\varepsilon \ll 1$. This method will therefore be applied in this paper.

2.2. Main results

Following Kolpakov (1991, 2004), Kalamkarov and Kolpakov (1997) and Buannic and Cartraud (2001) the main steps of the homogenization method with $e \to 0$ and $\varepsilon \to 0$ simultaneously are given in this section. The two small parameters are of the same order of magnitude and are assumed to be equal. Thus, the asymptotic expansion method with one small parameter can be used. The starting point of the method is the three-dimensional elasticity problem. Two scales are introduced: a *microscopic* one, which is the scale of the heterogeneities and of the width of the cross-section, and a *macroscopic* scale on which the size of the basic cell is very small. The corresponding variables are respectively y_i x_i/ε and x_3 where $\boldsymbol{x}$ (x_1, x_2, x_3) is the initial three-dimensional variable as shown in Fig. 1. The operators of the three-dimensional elasticity problem are then expressed as functions of these new variables. Next, the solution is searched under the form

$$u(x) = u_\alpha^0(x_3)e_\alpha + \varepsilon u^1(x_3, y_1, y_2, y_3) + \varepsilon^2 u^2(x_3, y_1, y_2, y_3) + \cdots \tag{1}$$

where functions $u^i(x_3, y_1, y_2, y_3)$ are periodic in variable y_3 with the period Y_3 (the length of the cell Y at the microscopic scale, see Fig. 1), which will be denoted Y_3-periodic.

It is usually considered that the first term $u^0(x_3)$ of the expansion in Eq. (1) has only components in direction e_1 and e_2 ($u_3^0 = 0$) which amounts to assuming that the bending is prominent. From Eq. (1), it turns out that the three-dimensional elasticity problem splits in a sequence (in powers of ε) of three-dimensional microscopic problems, posed on the basic cell, and one-dimensional macroscopic problems providing the overall beam response.

Considering Kolpakov (1991, 2004), Kalamkarov and Kolpakov (1997) and Buannic and Cartraud (2001), the main results of the method are now recalled

- The solution of the leading order (-1th order) microscopic problem is (the solution is unique up to a Y_3-periodic rigid body displacement, which is the composition of a e_3 axis rotation φ^1 and a translation $\hat{u}_1$):

$$u^1 = -y_\alpha \partial_3 u_\alpha^0(z_3)e_3 + \hat{u}^1(z_3) + \varphi^1(z_3)(y_1 e_2 - y_2 e_1) \tag{2}$$

where ∂_3 denotes $\partial/\partial x_3$.
- The leading order macroscopic problem corresponds to an anisotropic Navier Euler Bernoulli Saint-Venant beam. This problem involves the axial displacement $\hat{u}_3^1$, the transverse displacements $\hat{u}_\alpha^0$ and the rotation φ^1 (see Fig. 2). The homogenized (or effective) constitutive relations are obtained from the solution of the 0th order microscopic problem presented in the next section.
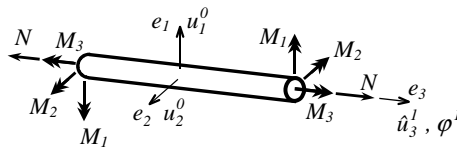

Fig. 2. Loading and displacements of a e_3 axis beam structure.

2.3. The basic cell problems

At the 0th order, the data of the microscopic problem come from the macroscopic strain of the displacement u^1 given in Eq. (2). The macroscopic variable x_3 being one-dimensional, one is led to introduce the components of the macroscopic strain (∂_{33} denoting $\partial^2/\partial x_3^2$)

$$
\begin{cases}
E^E(x_3) = \partial_3 \hat{u}_3^1(x_3) \\
E^{C_\alpha}(x_3) = \partial_{33} u_\alpha^0(x_3) \\
E^T(x_3) = \partial_3 \varphi^1(x_3)
\end{cases}
\tag{3}
$$

which correspond respectively to extension, curvatures, and torsion rate. Denoting a the elastic moduli tensor, div_y and ε_y the divergence and strain operators with respect to the microscopic variable y, and ∂Y_ℓ the lateral surface of the period (see Fig. 1), the basic cell problems consist in finding the fields u^{per}, ε, σ such that:

$$
\begin{cases}
\mathrm{div}_y \sigma = 0 \\
\sigma = a(y) : e \\
e_{\alpha\beta} = e_{y_{\alpha\beta}}(u^{\mathrm{per}}) \\
e_{13} = e_{y_{13}}(u^{\mathrm{per}}) - y_2 E^T/2 \\
e_{23} = e_{y_{23}}(u^{\mathrm{per}}) + y_1 E^T/2 \\
e_{33} = e_{y_{33}}(u^{\mathrm{per}}) + E^E - y_\alpha E^{C_\alpha} \\
\sigma.n = 0 \text{ on } \partial Y_\ell \\
u^{\mathrm{per}} \text{ per and } \sigma.n \text{ anti-per}
\end{cases}
\tag{4}
$$

where 'per' means Y_3-periodic in variable y_3, and anti-per means that $\sigma.n$ are opposite on opposite sides ∂Y^- and ∂Y^+ in the beam axis direction. Due to the linearity of Eq. (4), its solution (up to a Y_3-periodic rigid body displacement field) is given by

$$
\begin{cases}
u^{\mathrm{per}} = \chi^E(y)E^E(x_3) + \chi^{C_\alpha}(y)E^{C_\alpha}(x_3) + \chi^T(y)E^T(x_3) \\
\sigma = \sigma^E(y)E^E(x_3) + \sigma^{C_\alpha}(y)E^{C_\alpha}(x_3) + \sigma^T(y)E^T(x_3)
\end{cases}
\tag{5}
$$

where the expressions of $\sigma^E, \sigma^{C_\alpha}, \sigma^T$ are easily obtained from $\chi^E, \chi^{C_\alpha}, \chi^T$ using Eq. (4)$_{2-6}$. The overall beam behavior is defined from the macroscopic beam stresses obtained through integration over the cross-section and averaging in period length. Let us introduce the macroscopic axial force $N(x_3)$, the bending moments $M_\alpha(x_3)$ and the torque $M_3(x_3)$ detailed in Fig. 2:

$$
\begin{cases}
N(x_3) = \langle \sigma_{33} \rangle; \quad M_\alpha(x_3) = \langle -y_\alpha \sigma_{33} \rangle; \quad M_3(z_3) = \langle -y_2\sigma_{13} + y_1\sigma_{23} \rangle \\
\langle \cdot \rangle = \frac{1}{Y_3} \int_Y .\, dy_1\, dy_2\, dy_3
\end{cases}
\tag{6}
$$

where Y_3 stands for the scaled length of period Y. The overall beam behavior is then defined with respect to $y_\alpha \quad 0$, this axis being defined as the mean-line of the periodic structures for our applications. The homogenized constitutive equation can then be put in the form

$$
\begin{Bmatrix} N \\ M_1 \\ M_2 \\ M_3 \end{Bmatrix} = [a^{\mathrm{hom}}] \begin{Bmatrix} E^E \\ E^{C_1} \\ E^{C_2} \\ E^T \end{Bmatrix}
\tag{7}
$$

where $[a^{\mathrm{hom}}]$ is symmetric and can be expressed from Eqs. (5, 6). Therefore, the overall behavior is obtained from the solutions of the basic cell problems.

To the knowledge of the authors, analytical solution of the three-dimensional problem given by Eq. (4) is not available for periodic beams. Some bounds of the effective stiffnesses can be obtained using variational principles as detailed by Kolpakov (1998). In this paper, the basic cell problem is solved using finite element method whose implementation is presented in the next section.

3. Numerical solving of homogenization problems

The basic cell problems given by Eq. (4) have the same characteristics as those dealt with for the homogenization of the elastic behavior of periodic composite materials (macroscopic deformation, periodicity conditions), and for which different finite element solution approaches are available in the literature, see Débordes et al. (1985), Devries et al. (1989), Guedes and Kikuchi (1990) and Michel et al. (1999) among others. Most often, the finite element method is used to solve the basic cell problems, and the discretized field is u^{per}. Then, in Eq. (4), if as in Devries et al. (1989) and Guedes and Kikuchi (1990), $\tau \quad a(y){:}e_y(u^{\mathrm{per}})$ is chosen as the stress unknown, accounting for the macroscopic strains leads to body forces and surface loads on the lateral surface of the period, and the calculation of the global force vector is therefore tedious. If, as in Débordes et al. (1985), the stress field is σ, one has to modify the strain displacement finite element relation in order to satisfy Eq. $(4)_{3\ 6}$.

In this paper, another approach is proposed. The discretized field being u, such as $e(u)$ is determined from Eq. $(4)_{3\ 6}$, which yields

$$\begin{cases} u_1 = u_1^{\mathrm{per}} + \frac{1}{2}y_3^2 E^{C_1} - y_2 y_3 E^T \\ u_2 = u_2^{\mathrm{per}} + \frac{1}{2}y_3^2 E^{C_2} + y_1 y_3 E^T \\ u_3 = u_3^{\mathrm{per}} + y_3 E^E - y_\alpha y_3 E^{C_\alpha} \end{cases} \tag{8}$$

In that way, the only specificity of the basic cell problems is to take into account the periodicity of the displacement u^{per}, which amounts to linear relationships between degrees of freedom of two nodes on opposite sides ∂Y and ∂Y^+ in the beam axis direction. Denoting U the degrees of freedom associated with u, these relations are given by

$$\begin{cases} U_1^{+} - U_1^{-} = Y_3(y_3 E^{C_1} - y_2 E^T) \\ U_2^{+} - U_2^{-} = Y_3(y_3 E^{C_2} + y_1 E^T) \\ U_3^{+} - U_3^{-} = Y_3(E^E - y_\alpha E^{C_\alpha}) \end{cases} \tag{9}$$

where $y_3 = (y_3^+ + y_3^-)/2$, $y_\alpha = y_\alpha^+ = y_\alpha^-$, and where the superscript $-$ and $+$ denotes respectively the two parts ∂Y and ∂Y^+ of the period boundary concerned with periodicity conditions, see Fig. 1. Such a method has already been used by Anthoine et al. (1997).

The basic cell problems are treated using Eq. (9), and by successively imposing a component of the macroscopic strain of Eq. (3) to be equal to unity, and the others to be zero. As an example, considering $E^E \quad 1$ and $E^{C_\alpha} = E^T = 0$, from Eqs. (5) and (8), the finite element analysis provides the solution $u_\alpha = \chi_\alpha^E, u_3 = \chi_3^E + y_3$ and $\sigma \quad \sigma^E(y)$.

The effective properties can then be computed using Eqs. (6, 7), the first column of $[a^{\mathrm{hom}}]$ being obtained. A more straightforward way to proceed consists of using the total strain energy of the period, since we have, from Eqs. (4) and (7)

$$\int_Y \sigma : e \, dY = Y_3 \begin{Bmatrix} N \\ M_1 \\ M_2 \\ M_3 \end{Bmatrix}^T \begin{Bmatrix} E^E \\ E^{C_1} \\ E^{C_2} \\ E^T \end{Bmatrix} = Y_3 \begin{Bmatrix} E^E \\ E^{C_1} \\ E^{C_2} \\ E^T \end{Bmatrix}^T [a^{\text{hom}}] \begin{Bmatrix} E^E \\ E^{C_1} \\ E^{C_2} \\ E^T \end{Bmatrix}$$

Thus, considering the problem with $E^E = 1$ and $E^{C_\alpha} = E^T = 0$, the strain energy leads to a_{11}^{hom}.

4. Stiffness of corrugated beams

4.1. Description of the problem

This part deals with two periodic structures with uniform in-plane constant square cross-section (area A and inertia I about the e_2-axis) corrugated beams, having zigzag and sinus mean-lines. The basic cell geometry (period length L, amplitude D, section side dimension) is shown in Fig. 3. These structures are subjected to in-plane loading with an axial force N and a bending moment M_2 (see Fig. 2). The overall static behavior is of the form

$$\begin{Bmatrix} N \\ M_2 \end{Bmatrix} = \begin{bmatrix} a_{11}^{\text{hom}} & a_{13}^{\text{hom}} \\ a_{31}^{\text{hom}} & a_{33}^{\text{hom}} \end{bmatrix} \begin{Bmatrix} E^E \\ E^{C_1} \end{Bmatrix}$$

4.2. Reference solution

Homogenization of such corrugated beams has been studied by Potier-Ferry and Siad (1992). Starting from curved beam equations accounting for the mean-line geometry, the double scale asymptotic expansion method is used. The effective properties of the equivalent straight beam are then derived. The stiffness terms are then expressed as follows:
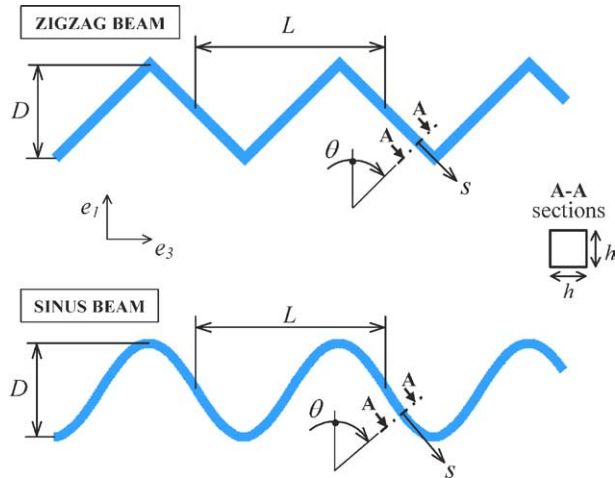

Fig. 3. Corrugated structures.

$$\begin{cases} a_{11}^{\text{hom}} = \dfrac{E\langle\langle\cos\theta\rangle\rangle}{\dfrac{\langle\langle\cos^2\theta\rangle\rangle}{A} + \dfrac{\langle\langle x_1^2\rangle\rangle}{I}} \\ a_{33}^{\text{hom}} = EI\langle\langle\cos\theta\rangle\rangle \\ a_{13}^{\text{hom}} = a_{31}^{\text{hom}} = 0 \end{cases}$$

E is Young's elasticity modulus, θ represents the cross-section inclination angle (measured with respect to the e_1-axis) as depicted in Fig. 3 and $\langle\langle\cdot\rangle\rangle$ is the average operator

$$\langle\langle f\rangle\rangle = \frac{1}{S}\int_S f\cdot\mathrm{d}s$$

with s being the curvilinear coordinate (see Fig. 3) and S being the length of one period beam's mean-line.

4.3. Homogenization results

For the present study, the following numerical values have been considered both for the zigzag and the sinus periodic beam: L 100 mm; D $L/2$; h 1 mm; E 200 GPa; v 0.3. Two three-dimensional FE models have been computed on SAMCEF code and coupled with the homogenization procedure described in section 2. The meshes (presented in blank in Fig. 4) are built using 4 finite elements per cross-sections, the corrugated beam period consists of a total of 526 finite 20-nodes solid elements (leading to 9122 dof).

The deformed shapes obtained for the displacement field u given by Eq. (8) are depicted in Fig. 4. The two cases depicted are obtained applying the following macroscopic strains:

- case (a), traction: $E^E = 1$; $E^{C_1} = E^{C_2} = E^T = 0$,
- case (b), bending: $E^{C_2} = 1$; $E^E = E^{C_1} = E^T = 0$.

Table 1 details the stiffness terms computed both using the homogenization procedure and the reference analytical solutions for the two corrugated beams. These numerical results appear to be consistent: the difference between analytical stiffness coefficients and those deducted from the homogenization approach are always less than 2%.
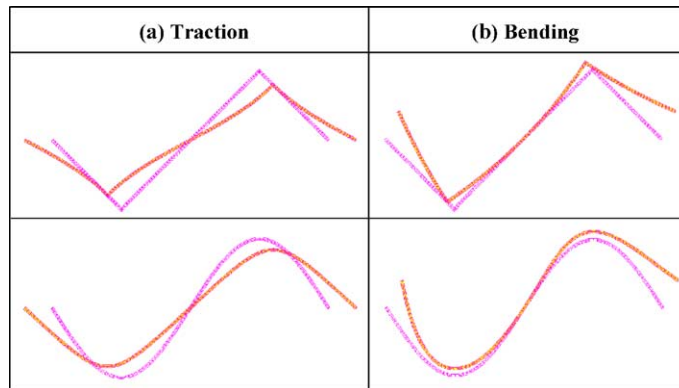

Fig. 4. Deformed/undeformed corrugated beams.

Table 1
Stiffness coefficients for the corrugated beams

		a_{11}^{hom} (N)	$a_{33}^{\text{hom}}(10^{-3} \text{ N m}^2)$
Zigzag beam	Homogenization	57.45	11.85
	Potier Ferry and Siad (1992)	56.56	11.79
Sinus beam	Homogenization	42.63	11.60
	Potier Ferry and Siad (1992)	42.64	11.39

5. Axial stiffness of a stranded cable

5.1. Description of the problem

This part deals with the static behavior of steel ropes widely employed for bridges and pre-stressed structures mentioned by Costello (1997), Labrosse (1998) and Nawrocki and Labrosse (2000). The studied cable are 'spiral strand $6 + 1$' type: six cylindrical wires are wrapped around a cylindrical straight core as illustrated in Fig. 5. The geometry is characterized by the core radius R_C, the strands radius R_S, and the helical angle α measured with respect to the cable e_3-axis. The strand cross-sections are elliptical in the (e_1, e_2) plane due to the helical α angle (see Fig. 5). The helical construction mode exhibits a periodic beam-like design, the length of one period being given by the following expression:

$$L = \frac{2\pi(R_C + R_S)}{\tan \alpha}$$

Such rope generally possesses anchorages at its ends allowing free rotations in the e_1 and e_2 radial directions (see Figs. 2 and 5) as mentioned by Nawrocki and Labrosse (2000). This study focusing on the axial behavior, the bending characteristics are not investigated. Due to the helical design of the strands, the overall axial behavior exhibits a coupling between tensile and torsion and can be expressed using the following 2×2 stiffness matrix:
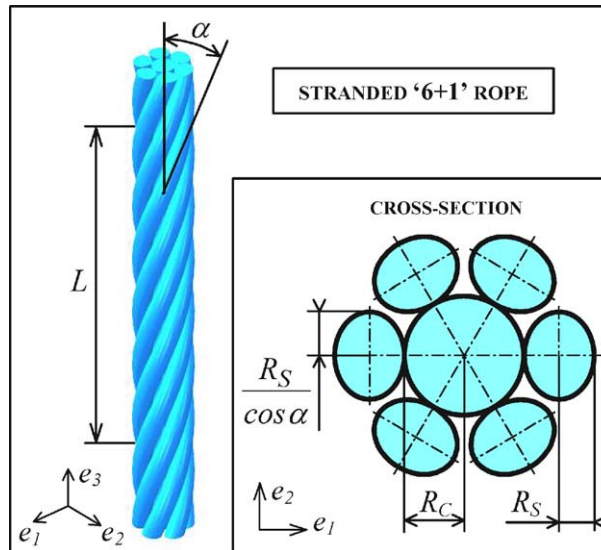

Fig. 5. Geometry of the cable.

$$\left\{ \begin{array}{c} N \\ M_3 \end{array} \right\} = \left[\begin{array}{cc} a_{11}^{\mathrm{hom}} & a_{14}^{\mathrm{hom}} \\ a_{41}^{\mathrm{hom}} & a_{44}^{\mathrm{hom}} \end{array} \right] \left\{ \begin{array}{c} E^E \\ E^T \end{array} \right\}$$

using the tensile and torsion stiffness coefficients terms a_{11}^{hom} and a_{44}^{hom} respectively, and the coupling coefficients $a_{14}^{\mathrm{hom}} = a_{41}^{\mathrm{hom}}$.

5.2. Reference solution

As detailed by Costello (1997), Labrosse (1998) and Roshan Fekr et al. (1999), many authors have proposed analytical expressions for stiffness coefficient a_{ij}^{hom} of stranded '6 + 1' cables. For the present work, Labrosse's stranded cable model has been used as a reference (see Labrosse (1998)). In this approach, the wires and the core are modeled as curved beams. The axial force, bending moments and torque on a cable cross section, as well as the inter-wire efforts are expressed as a function of the cable strains and derivative of the inter-wire slippage.

The influence of relative inter-wire motions on the cable overall response has been discussed by Nawrocki and Labrosse (2000). All the possible cases of inter-wire contacts have been studied, and the results demonstrate that rolling and sliding have no influence on the overall behavior. Moreover, the comparison with experimental data shows that the pivoting has to be considered as free. It is therefore possible to describe the kinematics of the cable section as a function of the degrees of freedom of the core. The overall behavior of the cable can thus be deduced from these of its constituents. Closed-form stiffness component expressions are then obtained

$$\begin{cases} a_{11}^{\mathrm{hom}} = \pi E (R_{\mathrm{C}}^2 + 6R_{\mathrm{S}}^2 \cos^3\alpha) \\ a_{44}^{\mathrm{hom}} = \pi E \left[\frac{1}{4(1+v)} (R_{\mathrm{C}}^4 + 6R_{\mathrm{S}}^4 \cos^5\alpha) + 6\cos\alpha \sin^2\alpha R_{\mathrm{S}}^2 \left((R_{\mathrm{C}} + R_{\mathrm{S}})^2 + \frac{R_{\mathrm{S}}^2}{4}(1 + \cos^2\alpha) \right) \right] \\ a_{14}^{\mathrm{hom}} = a_{41}^{\mathrm{hom}} = 6\pi E R_{\mathrm{S}}^2 (R_{\mathrm{C}} + R_{\mathrm{S}}) \cos^2\alpha \sin\alpha \end{cases}$$

5.3. Homogenization results

The homogenization procedure has been applied for the example treated by Nawrocki and Labrosse (2000) validated by experiments (see Labrosse, 1998). The cable geometry is given by (in mm) R_{C} 2.675, R_{S} 2.59 and L 230.13 then leading to α 8.18°. The constitutive material is characterized by: E 200 MPa; v 0.3.

Following the homogenization procedure principle detailed in section 2, only one three-dimensional period of the cable has been modeled using Samcef FEM code as illustrated in Fig. 6. It is worth to notice that the geometry of the strands has been generated exactly by extruding circular surfaces along the centroidal helical curves of the wires: as shown by Roshan Fekr et al. (1999), geometrical approximation (i.e., circular strand cross-sections in the (e_1, e_2) plane instead of the real elliptical geometry, see Fig. 4) have a great influence on numerical results.

As illustrated in Fig. 6, each wire sections is modeled using 12 finite elements (six 16-nodes and six 12-nodes solid elements), leading to a total of 7056 finite elements and 52,049 dof. For the α angle value considered, each solid element exhibits small shape distortion. Within the framework of a preliminary study detailed in Ghoreishi et al. (2004), the influence of inter-wire contact conditions between the strands and the core has been studied for two limit cases: sliding without friction and merging. The results obtained show that the static overall behavior is not sensitive to these modeling assumption. For the present study, each cross-section of the core is therefore merged to those of the strands using 6 common nodes as depicted in Fig. 5. This assumption is consistent with the classical theoretical framework of homogenization which implies that the basic cell constituents are assumed to be perfectly bonded.
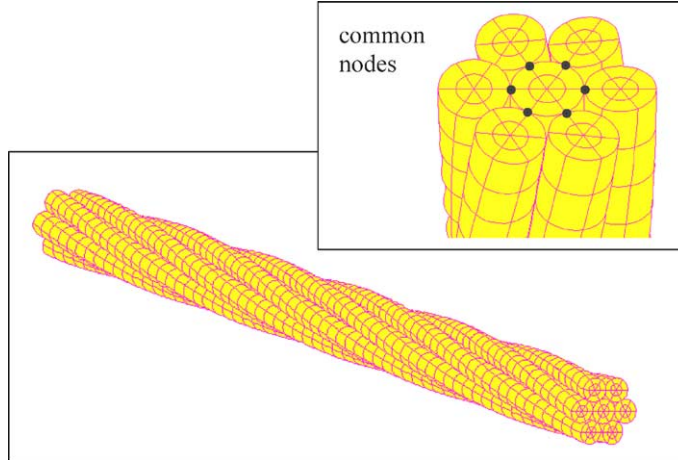
Fig. 6. Three dimensional FEM model of the cable.

Table 2
Stiffness coefficients for the stranded '6+1' cable

	a_{11}^{hom} (10^6 N)	a_{44}^{hom} (N m^2)	a_{14}^{hom} (10^6 N m)
Homogenization	28.63	53.49	1.824
Labrosse (1998)	29.02	52.91	1.856

The stiffness values obtained both using the three-dimensional FE model coupled to the homogenization procedure and Labrosse's analytical model are given in Table 2. As can be seen, the homogenization procedure leads to accurate predictions: the corresponding stiffness coefficients present very small differences (always below 2%) with the analytical reference solutions. These results therefore corroborate and validate the homogenization results.

6. Conclusion

In this work, the homogenization theory is applied to beams with periodic microstructure. A finite element implementation of basic cell problems is presented. This method is based on a three-dimensional model, and can be easily used with a standard finite element software.

Numerical investigations carried out for two corrugated beams and a stranded '6 + 1' cable have demonstrated the accuracy of this approach for stiffness predictions with respect to reference solutions of the literature. Moreover, it can be underlined that the homogenization computations have required few CPU times (always less than 2 min) on a standard workstation. These numerical examples allow to validate the efficiency and usefulness of the homogenization procedure.

References

Anthoine, A., Guedes, J., Pegon, P., 1997. Non linear behavior of reinforced concrete beams: from three dimensional to 1D member modeling. Computers and Structures 65 (6), 949 963.

Buannic, N., Cartraud, P., 2001. Higher order effective modelling of periodic heterogeneous beams Part I: Asymptotic expansion method. International Journal of Solids and Structures 38, 7139 7161.

Caillerie, D., 1984. Thin elastic and periodic plates. Mathematical Methods in Applied Sciences 6, 159 191.

Cioranescu, D., Saint Jean Paulin, J., 1999. Homogenization of Reticulated Structures. Applied Mathematics Science. Springer, New York.

Costello, G.A., 1997. Theory of Wire rope, second ed. Springer, Berlin.

Débordes, O., Licht, C., Marigo, J.J., Mialon, P., Michel, J.C., Suquet, P., 1985. Calcul des charges limites de structures fortement hétérogènes . In: Grellier, J.P. (Ed.), Tendances actuelles en calcul des structures, Pluralis, Paris, pp. 56 70.

Devries, F., Dumontet, H., Duvaut, G., Léné, F., 1989. Homogenization and damage for composite structures. International Journal of Numerical Methods in Engineering 27, 285 298.

Geymonat, G., Krasucki, F., Marigo, J.J., 1987. Sur la commutativité des passages à la limite en théorie asymptotique des poutres composites. Comptes Rendus de l'Académie des Sciences I 305 (2), 225 228.

Ghoreishi, R., Messager, T., Cartraud, P., Davies, P., 2004. Assessment of cable models for synthetic mooring lines. In: Proceedings of the 14th International Offshore and Polar Engineering Conference and Exhibition, ISOPE, Toulon, France.

Guedes, J.M., Kikuchi, N., 1990. Preprocessing and postprocessing for materials based on the homogenization method with adaptative finite element methods. Computer Methods in Applied Mechanical Engineering 83, 143 198.

Kalamkarov, A.L., Kolpakov, A.G., 1997. Analysis, Design and Optimization of Composite Structures. Wiley, Chichester.

Kolpakov, A.G., 1991. Calculation of the characteristics of thin elastic rods with a periodic structure. Journal of Applied Mathematics and Mechanics 55 (3), 358 365.

Kolpakov, A.G., 1998. Variational principles for stiffnesses of a non homogeneous beam. Journal of the Mechanics and Physics of Solids 46 (6), 1039 1053.

Kolpakov, A.G., 2004. Stressed Composite Structures: Homogenized Models for Thin walled Non homogeneous Structures with Initial Stresses. Springer Verlag, Berlin, New York.

Labrosse, M., 1998. Contribution à l'étude du rôle du frottement sur le comportement et la durée de vie des câbles monocouches. Ph.D Thesis, University of Nantes.

Michel, J.C., Moulinec, H., Suquet, P., 1999. Effective properties of composite materials with periodic microstruture: a computational approach. Computer Methods in Applied Mechanical Engineering 172 (1 4), 109 143.

Nawrocki, A., Labrosse, M., 2000. A finite element model for simple straight wire rop strands. Computers and Structures 77, 345 359.

Noor, A.K., 1988. Continnum modeling for repetitive lattice structures. Applied Mechanics Reviews 41 (7), 285 296.

Potier Ferry, M., Siad, L., 1992. Homogénéisation géométrique d'une poutre ondulée (Geometrical homogenization of a corrugated beam). Comptes Rendus de l'Académie des Sciences 314 (II), 425 430.

Roshan Fekr, M., McClure, G., Farzaneh, M., 1999. Application of Adina to stress analysis of an optical ground wire. Computers and Structures 72, 301 316.

Stephen, N.G., Wang, P.J., 1996. On Saint Venant's principle in pin jointed frameworks. International Journal of Solids and Structures 33 (1), 79 97.

Trabucho, L., Viano, J.M., 1996. Mathematical modelling of rods. In: Ciarlet, P.G., Lions, J.L. (Eds.), Handbook of Numerical Analysis. North Holland, Amsterdam, pp. 487 973.

Volovoi, V.V., Hodges, D.H., Berdichevsky, V.L., Sutyrin, V.G., 1999. Asymptotic theory for static behavior of elastic anisotropic I beams. International Journal of Solids and Structures 36 (7), 1017 1043.